Pak. J. Agri. Sci., Vol. 57(5), 1327-1335; 2020
ISSN (Print) 0552-9034, ISSN (Online) 2076-0906
DOI:10.21162/PAKJAS/20.111
http://www.pakjas.com.pk

NEAR REAL TIME FLOOD FORECASTING IN THE TRANSBOUNDARY CHENAB RIVER USING GLOBAL SATELLITE MAPPING OF PRECIPITATION

Sikandar Ali[1, *], Muhammad Jehanzeb Masud Cheema[1], Allah Bakhsh[1], Tasneem Khaliq[2]

[1]Department of Irrigation and Drainage, University of Agriculture, Faisalabad, Pakistan; [2]Department of Agronomy, University of Agriculture, Faisalabad, Pakistan
***Corresponding author's e-mail: sikandar_ali@uaf.edu.pk**

Floods are the most significant natural hazards worldwide, claim precious lives and cause serious damage to buildings, infrastructure and agricultural crops. Pakistan is also frequently suffering huge agro-economic dents and life loss by floods in Indus, Jhelum and Chenab rivers due to lack of budget, effective flood preparedness and flood forecasting. The flood forecasting in the Chenab river is a major challenge due to lack of hydrometeorological data as most of its catchment is under Indian control. In this study, three high spatiotemporal Global Satellite Mapping of Precipitation (GSMaP) products, GSMaP_Near Real Time (NRT), GSMaP_now (NOW) and GSMaP_RIKEN Nowcast (RNC) were used along with the global temperature, snow, landuse and soil datasets in Hydrologic Engineering Center-Hydrologic Modeling System (HEC-HMS) model for flood forecasting. The Soil Moisture Accounting (SMA) and temperature index methods were used for direct runoff estimation and snowmelt runoff modeling, respectively. The results revealed that GSMaP_NRT, GSMaP_NOW and GSMaP_RNC based simulated flow has Nash and Sutcliffe Efficiency (NSE) value of 0.58, 0.73 and 0.35, respectively, from 2017 to 2018. The GSMaP_NOW precipitation estimate has fair flow simulation results while the GSMaP_RNC product has poor simulation results. It is concluded from the results that GSMaP_NRT is a reliable high spatiotemporal precipitation estimate for hydrological studies and flood forecasting in data scarce Chenab river catchment.
Keywords: Transboundary River, Chenab, GSMaP, HEC-HMS, Flood Forecasting, Agricultural Crops.

INTRODUCTION

Floods are the most ruinous natural catastrophes among all the natural disasters (Stefanidis and Stathis, 2013) and cause various socio-economic skirmishes (Ghimire *et al.*, 2015). Floods affected more than 8 million people in the 20th century worldwide (Haynes *et al.*, 2009), disturbed livelihoods of about 520 million people and claimed 25000 lives annually across the world (Simonovic, 2009). In Pakistan, the super flood destroyed about 5.189 million acres of agricultural land in 2010 and caused huge economic loss to the country (OA, 2010). The Chenab river flood affected 2.415 million acres of standing crops in 2014 mainly covering cotton, rice, sugarcane and vegetables with direct damage to a large number of water channels and wells (FFC, 2017). Due to 2010 flood, the major crops like rice, wheat, cotton and sugarcane led to a declined growth of -4% and the overall agriculture sector recorded modest growth of 2.1% against the target of 3.8% (Looney, 2012) which caused huge economic dent and significant recovery cost. The research conducted by Multihazard Mitigation Council and United Nations Development Programme reveals that the money spent on the development of early warning system is inexpensive than the recovery cost (MMC, 2005; UNDP, 2012). Improvement in flood forecasting mechanism is one of the most effective forms of non-structural approaches which could offer a vital role in flood preparedness and disaster management (Yang *et al.*, 2015).

Real time flood forecasting is a major challenge to the researchers worldwide due to prevailing conditions over the high altitude complex river basins which are influenced by both the sensitivity of hydrologic models and climatic information of the area (FFC, 2000; Groisman *et al.*, 2004; Tariq and Giesen, 2012). The flood forecasting in the transboundary river, like the Chenab river, is more complicated due to delay of data transmissions among the users (Biemans *et al.*, 2009) especially in the snow dominant catchments (Herold *et al.*, 2016). The HEC-HMS model can simulate the river flows based on any individual precipitation event or continuous time period. Several hydrologic models have been applied in the river basins for event-based and continuous streamflow simulation across the globe (Anderson *et al.*, 2002; Cydzik and Hogue, 2009; De Silva *et al.*, 2014; Teng *et al.*, 2018; Ouédraogo*et al.*, 2018; Dariane*et al.*, 2020). The HEC_HMS model can also be applied for flood forecasting, flood frequency, system planning and early warning in the complex river basins (HEC, 2015). The SMA and temperature index are the suitable methods for loss estimation and snowmelt runoff modeling, respectively, in

HEC-HMS model (Sintayehu, 2015; García *et al.*, 2008; Wallner *et al.*, 2012).

The flood forecasting cannot be performed without estimation of relatively highly accurate precipitation estimates (Yang *et al.*, 2015) which is the key parameter among all the meteorological parameters (Tapiador *et al.*, 2012). Due to sparse network of raingauge stations and absence in high-altitude areas of the world (Immerzeel *et al.*, 2012), there is a need to use timely available satellite precipitation for flood forecasting. There are precipitation estimates derived from the constellation of passive microwave radiometers working on low-earth orbiting satellites and often merging data from geostationary infrared datasets for minimizing temporal uncertainties (Huffman *et al.*, 2007). The GSMaP is the project established by the Japan Science and Technology Agency and Japan Aerospace Exploration Agency to produce global precipitation at a spatial resolution of 0.25° and 0.1° using merged microwave radiometer and precipitation radar algorithms. The project aims to develop an advanced microwave algorithm which is based on a deterministic rain retrieval algorithm (Aonashi *et al.*, 2009) based on physical precipitation models consisting of particle size distribution and melting layers. (Kubota *et al.*, 2007).

Flood forecasting of the transboundary Chenab river is a major challenge due to lack of hydrometeorological data of its catchment. In case of Chenab river, Pakistan is at downstream and being an agricultural country timely information of floods is very crucial for agricultural water management. In this study, an innovative and comprehensive approach is discussed to forecast floods in the Chenab river using satellite-based precipitation estimates. The three high spatiotemporal GSMaP precipitation estimates were integrated into the HEC-HMS model for flood forecasting of the Chenab river. The event-based and continuous simulation was performed using global temperature, snow depth, snow density, landuse and soil datasets along with the GSMAP precipitation estimates. The accuracy of flood forecasting was assessed by statistical comparison between the observed and simulated flows at the outlet (Marala barrage).

MATERIALS AND METHODS

***Study Area*:** The Chenab river catchment lies in the geographic coordinate range of 74º to 77.83º E longitude and 32.1º to 34.1º N latitude with an elevation range of 224m to 7085m above mean sea level as shown in figure 1. The Chenab river originates from the Lahul-Spiti district of India, enters Jammu and Kashmir in Kishtwar district and then flows towards Pakistan in Sialkot district by covering a total length of about 590 km from its origin point to the outlet. For modeling purpose, the catchment of Chenab river is divided into 20 subbasins for hydrological modeling as shown in figure 1. The high-altitude of the catchment receives heavy snow and extreme precipitation in winter and summer season, respectively. The monsoon season is overlapped with the summer season which can cause extreme floods in the Chenab river due to heavy precipitation and snowmelt at the same time in its catchment.

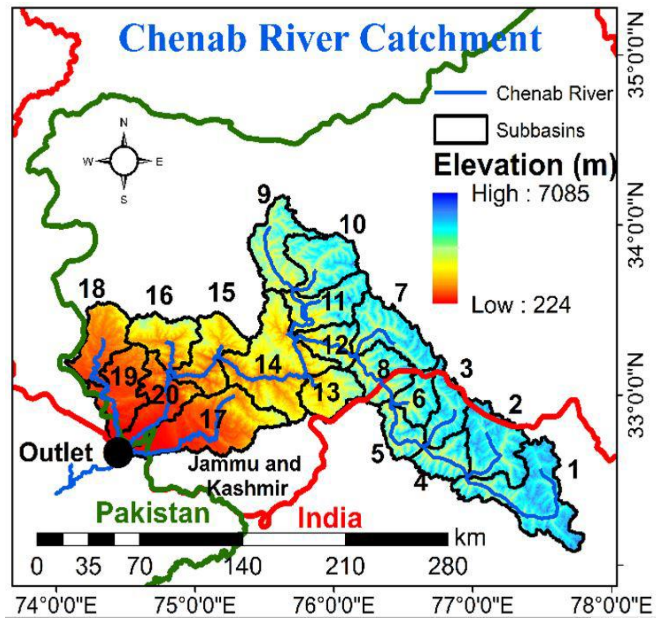

Figure 1. Chenab River and its Subbasins (1-20).

***Datasets used in the study*:** In this study, precipitation estimates with different temporal resolutions and latency periods were incorporated in the HEC-HMS model for simulating the daily Chenab river flow. The GSMaP is the highly precise and high spatiotemporal resolution precipitation estimate consisting of extensive satellite information from both infrared and passive microwave radiometer (Okamoto *et al.*, 2005; Kubota *et al.*, 2007; Aonashi *et al.*, 2009; Ushio *et al.*, 2009). The first precipitation estimate GSMaP_NRT was used in the study with a spatial resolution of 0.1º on hourly timespans with a very low latency period which is the core cause for its use in monitoring the hydrological response in the river basins. The GSMaP_NRT precipitation estimate has various input data sources (Ebert *et al.*, 2007) and offering its availability to the public since 2002. The GSMaP_NOW half-hourly precipitation estimate is also used with the same spatial resolution extrapolated by 0.5-hour using cloud motion vector and updated by every 30 minutes for water resources and flood management studies (Tsujimoto *et al.*, 2014). The GSMaP_RNC precipitation forecast provides data for the next 12 hours (OTSUKA *et al.*, 2019) which could be used effectively for flood forecasting. The GSMaP_RNC is formulated by the extrapolation of GSMaP_NRT using the cloud motion vector patterns. The latency period of GSMaP_NRT and GSMaP_NOW precipitation product is 4 and 1 hour, respectively, (Kubota *et al.*, 2017; Tang *et al.*,

2017) while GSMaP_RNC forecasts precipitation 12 hours in advance.

The daily Climate Prediction Center (CPC) temperature dataset with a spatial resolution of 0.5º was incorporated in the study for snowmelt runoff modeling in HEC-HMS model. The CPC temperature dataset is formulated by more than 30,000 gauge reports obtained from multiple National and International organizations of the world (Xie *et al.*, 2007). In addition, Moderate Resolution Imaging Spectroradiometer (MODIS) temperature information (MOD11A1) was also blended with the CPC temperature product at a spatial resolution of 0.5° for snowmelt runoff modeling. The European Centre for Medium-Range Weather Forecasts (ECMWF) Re-Analysis 5 (ERA5) was used (Hersbach and Dee, 2016) to estimate the snow properties over the river catchment and SWE was estimated using the equation (Sturm *et al.*, 2010):

$$SWE = SD\frac{\rho_s}{\rho_w}$$

where, SD is snow depth, ρ_b is the density of snow and ρ_w is the density of water.

***Soil moisture accounting method*:** The SMA method was used in the HEC-HMS model for retention by vegetative cover and simulation of water movement to the groundwater through soil layers (Feldman, 2000). The SMA algorithm describes the watershed in the series of storage layers as shown in figure 2.

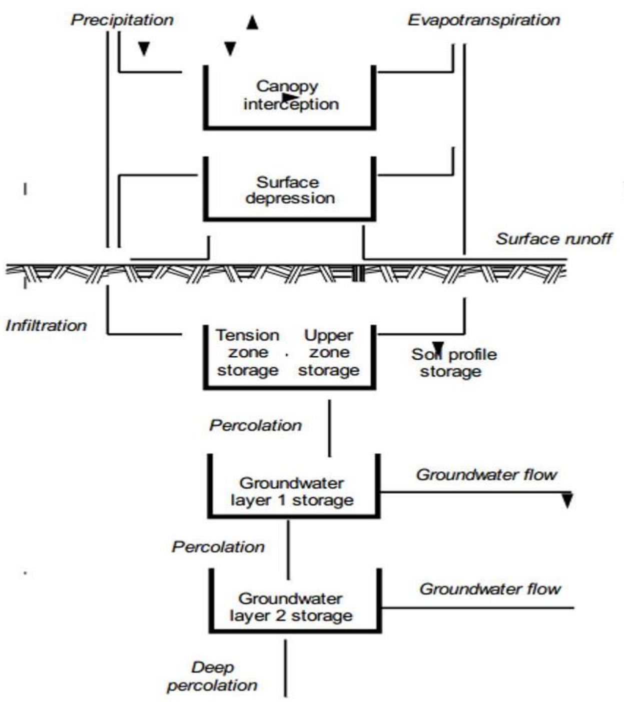

Figure 2. Description of Soil Moisture Accounting method (Feldman, 2000).

The soil layers give wetting and recovery cycles for simulation of the watersheds which requires the initial soil moisture conditions of the subbasins (Alexakis*et al.*, 2017; Bhuiyan *et al.*, 2017). As most of the watershed of the Chenab river lies in Indian control as shown in figure 1, so alternate sources of information were incorporated for the catchment. The initial values for canopy storage, surface storage and tension storage were fixed by keeping in view the range mentioned in HEC-HMS technical reference manual (Schaffenberg and Fleming, 2006). The daily MODIS (MOD09GA) imagery and landuse of the European Space Agency (ESA) were also used in order to keep the initial values within the limits. The values of maximum infiltration, imperviousness, soil storage and soil percolation were extracted from the Food and Agriculture Organization (FAO) soil database, ESA landuse and daily MOD09GA product. The Soil Conservation Services (SCS) unit hydrograph, lag time and constant monthly methods were used for estimation of direct runoff, routing and baseflow, respectively.

***Temperature index method*:** The temperature index method was used in HEC-HMS model for simulating the snowmelt runoff (Fazel *et al.*, 2013; Razmkhah, 2016; Dariane*et al.*, 2020), which defines the subbasin precipitation as either liquid water or frozen snow by defining a temperature threshold. The melted water acts as hyetograph for the corresponding subbasin and thereby contributes to the streamflow. The temperature index method represents cold energy stored in the snowpack (SWE) with past conditions and all the other factors for estimation of melting for each degree above freezing temperature. Every subbasin is divided into different elevation bands by using Advanced Spaceborne Thermal Emission and Reflection Radiometer Digital Elevation Model.

For calibration of the model, event-based calibration was carried out for 4 events occurring between 2017 and 2018 using SMA and temperature index methods. Initially, the automatic and manual calibration was applied for fixation of all the SMA and temperature index parameters. Afterward, the continuous snowmelt runoff simulation was carried out for the complete timespan ranging from 2017 to 2018. The simulated and observed flows were compared for accuracy assessment using the statistical approaches like Coefficient of Determination (R^2), Pearson r and NSE.

RESULTS

The first event was simulated from 29-01-2017 to 14-02-2017 using all the mentioned GSMaP precipitation estimates. The results in figure 3, supported by Table 1, show that there is a very poor agreement between the observed and simulated flow for GSMaP_RNC precipitation product. Whereas, the other 2 precipitation estimates show fair results with underestimation at peak observed flow time. The higher values of R^2, Pearson r and NSE for GSMaP_NOW based

Table 1. Statistical comparison of GSMaP products based simulated flows with the observed flow for all the 4 events.

Function	Event-1			Event-2			Event-3			Event-4		
	GSMaP _NOW	GSMaP _NRT	GSMaP _RNC	GSMaP _NOW	GSMaP _NRT	GSMaP _RNC	GSMaP _NOW	GSMaP _NRT	GSMaP _RNC	GSMaP _NOW	GSMaP _NRT	GSMaP _RNC
R^2	0.97	0.92	0.63	0.94	0.90	0.89	0.89	0.92	0.83	0.89	0.92	0.85
Pearson r	0.99	0.91	0.42	0.52	0.20	-0.07	0.63	0.77	0.39	0.37	0.54	-0.13
NSE	0.63	-0.23	-0.09	-0.52	-1.37	-2.2	0.37	0.49	-0.01	-0.41	0.02	-1.57

flow simulation also indicate fair simulation results as compared to GSMaP_NRT based simulation results.

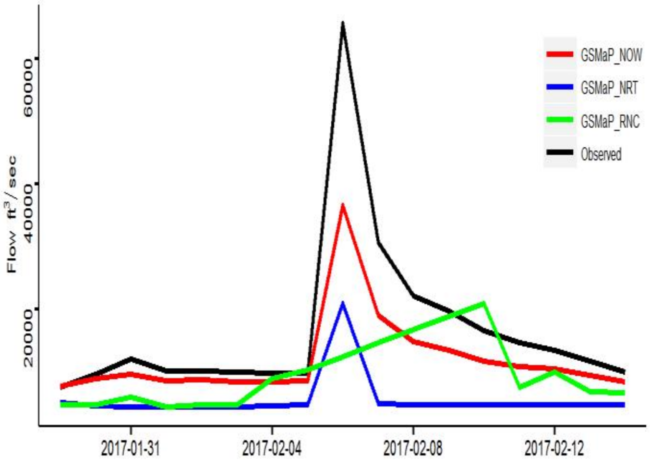

Figure 3. Simulated and observed flow comparison for event-1.

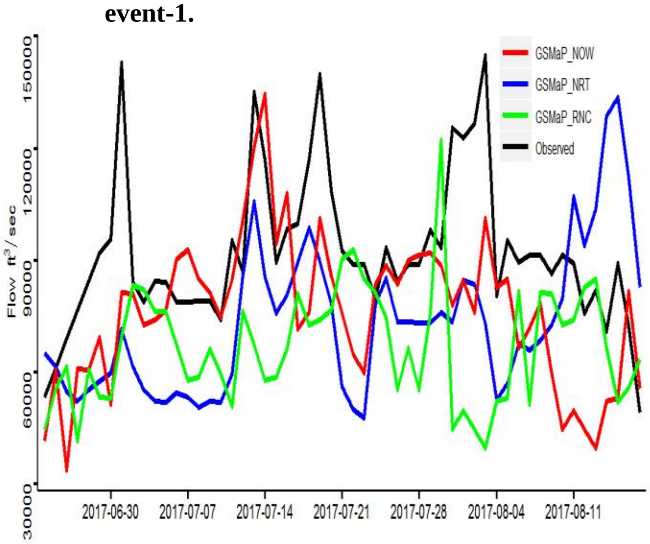

Figure 4. Simulated and observed flow comparison for event-2.

The second event was simulated for the time period ranging from 24-06-2017 to 17-08-2017, the results in figure 4 and Table 1 show a reliable agreement for GSMaP_NOW based simulation as compared to the other 2 simulations. The higher values of NSE for GSMaP_NOW based simulated flow also indicate reliable results. The GSMaP_NRT based simulation shows slightly fair results with underestimated simulated flow over most of the event time while poor results were obtained for GSMaP_RNC based simulation.

The third event was simulated from 26-06-2018 to 07-07-2018, figure 5 shows a very poor simulation response for GSMaP_RNC precipitation estimate, while the simulated flows of the other 2 precipitation products are following the pattern of observed flow except at peak flow time. The higher NSE value (0.49) of GSMaP_NRT based simulated flow is indicating fair results as compared to the GSMaP_NOW based simulation which is more deviating from the observed flow with NSE value of 0.37.

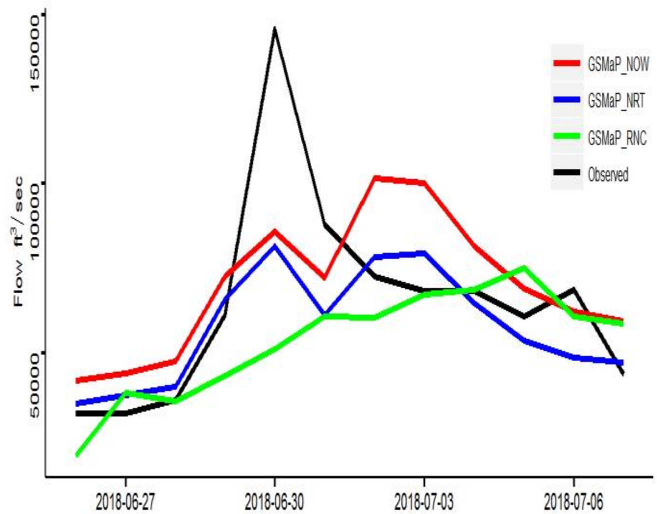

Figure 5. Simulated and observed flow comparison for event-3.

The fourth event was simulated from 04-08-2018 to 28-08-2018, figure 6 shows that there is good agreement of GSMaP_NRT based simulated flow with the observed flow as compared to the other 2 flow simulations. The GSMaP_NOW based simulated flow is under and overestimating the observed flow with lower values of R^2, Pearson rand NSE. While, the result of GSMaP_RNC based simulated flow is very poor with high underestimation revealing lower values of R^2, Pearson r and NSE. All the four events were used for calibrating the model and the automatic calibration performed well which provided information about the catchment behavior.

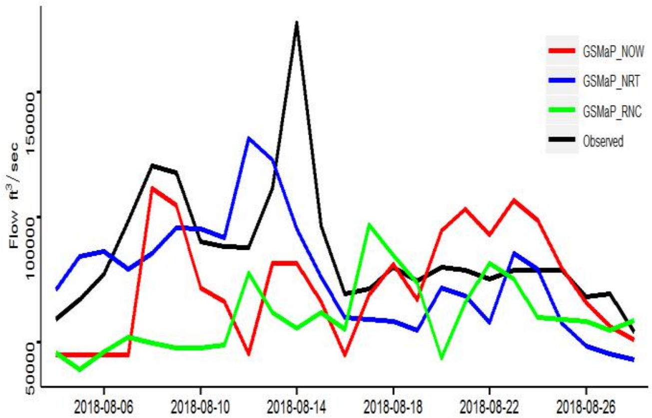

Figure 6. Simulated and observed flow comparison for event-4.

The calibrated model was further applied for long term continuous snowmelt modeling from 2017 to 2018 for all the mentioned GSMaP precipitation estimates. The results are presented in figure 7 (a-f), figures a, b and c are the time series plots for GSMaP_NOW, GSMaP_NRT and GSMaP_RNC based simulated flows, respectively. The figure 7 (d, e and f) shows statistical comparison, supported by Table 2, for GSMaP_NOW, GSMaP_NRT and GSMaP_RNC simulation, respectively. The GSMaP_NRT based simulated flow shows good agreement with the observed flow and it is also tested over the Indus basin by Sugiura *et al. (*2016). The GSMaP_NOW based simulated flow shows a slightly fair agreement with the observed flow for most of the timespan except for the peak flow time. In the summer of 2017, GSMaP_NOW simulation shows 1 peak while observed flow has three high magnitude flows and there is also variation in temporal occurrence of peak flow for summer season in 2018 as well. The GSMaP_RNC based simulated flow shows a very poor agreement with the observed flow with high over and underestimation for the entire time period of the simulation. The apparent reason for overestimation in precipitation magnitudes of GSMaP_RNC in tropics is due to overestimation of precipitation magnitudes by GSMaP_NRT (Kotsuki *et al.*, 2019).

From figure 7 (b, c, e and f) the overestimation and underestimation of GSMaP_NRT and GSMaP_RNC based

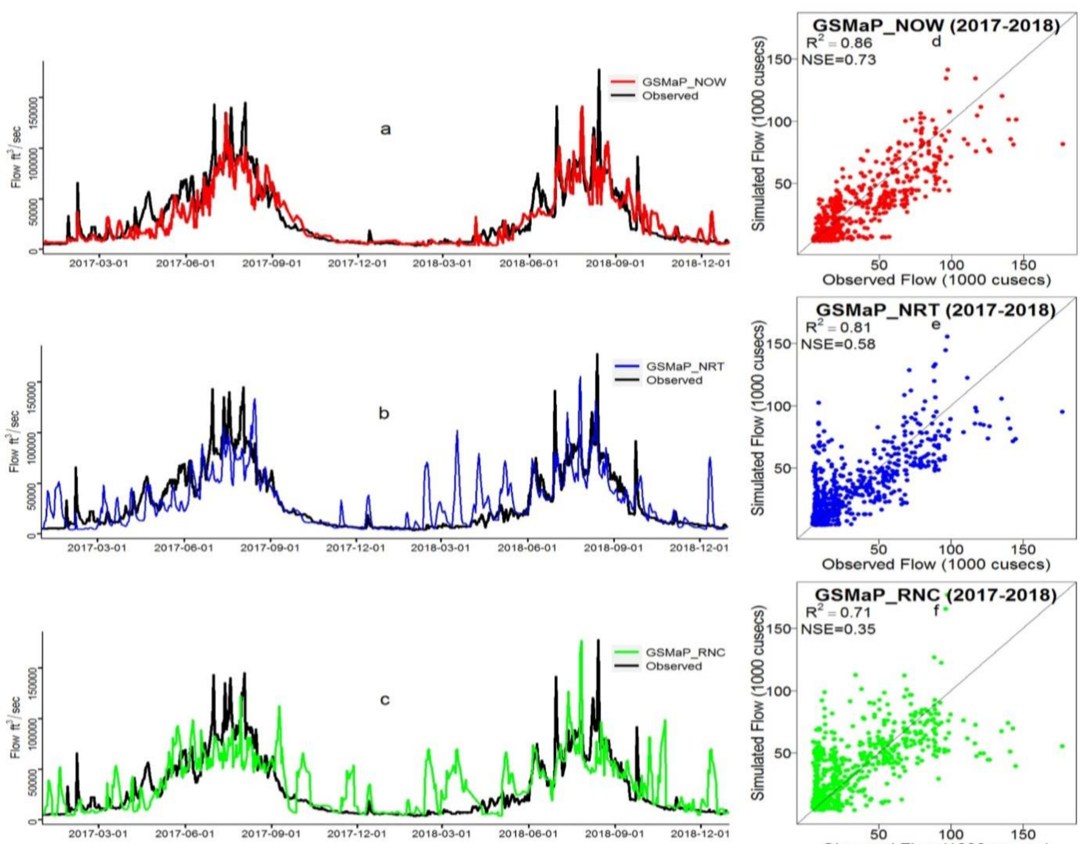

Figure 7 (a-f). Simulated and observed flow comparison for all the GSMaP Products. The figure a, d represents GSMaP_NOW simulation, figure b, e represents GSMaP_NRT simulation and figure c, f represents GSMaP_RNC simulation.

simulated flows can also be observed with higher variations in the latter. The statistics in figure 7 (d-f) and Table 2 reveal that R^2 and Pearson r values are higher for all the simulated flows indicating reasonable reliability of GSMaP precipitation estimates for time series simulation. The GSMaP_NOW based simulated flow has the highest NSE which indicates fair comparison for most of the time periods with small variations persistently occurring in the entire timespan as can be seen in figure 7 (d). The variations in GSMaP_NRT based simulated flow can be seen for less number of days in figure 7 (e and f), with lower but reliable NSE value. The R^2 and Pearson r values for GSMaP_NRT based simulation are also reliable indicating a good precipitation source. The statistics of GSMaP_RNC based simulated flow indicates a very poor value of NSE, thereby indicating a poor precipitation forecast.

Table 2. Statistical comparison of GSMaP products based simulated flows with the observed flow from 2017 to 2018.

Function	GSMaP_ NOW	GSMaP NRT	GSMaP RNC
R^2	0.86	0.80	0.71
Pearson r	0.85	0.77	0.65
NSE	0.73	0.58	0.35

DISCUSSION

The automatic calibration is an iterative approach used in the HEC-HMS model to reduce the uncertainty by optimizing the objective function which ultimately would reflect a good agreement between simulated and observed flows (Schaffenberg, 2013; Sintayehu, 2015; Majidi and Shahedi, 2012). The high spatiotemporal GSMaP_NRT, GSMaP_NOW and GSMaP_RNC precipitation products were used as input to the HEC-HMS model which are being applied worldwide (Aonashi *et al.*, 2009; Ushio *et al.*, 2009; Nakayama, 2015). For snow-related estimations, ERA-5 has been used by the researchers for cryosphere and flood studies across the globe (Terzago *et al.*, 2019; Tei *et al.*, 2019; Hersbach and Dee, 2016). The CPC and MODIS based temperature datasets were used in this research which are being used by the researchers due to their good results across the globe (Xu *et al.*, 2013; Mallakpour and Villarini, 2015; Corbari and Mancini, 2014; Kwak and Park, 2019). The SMA method is also suitable for event based modeling (Bhuiyan *et al.*, 2017) and long-time continuous hydrological modeling over the complex watersheds (Gyawali and Watkins, 2012; Singh and Jain, 2015). The SCS unit hydrograph method for estimation of direct runoff and lag time approach for routing was used in this study as recommended by the researchers worldwide (Verma *et al.*, 2010; Majidi and Shahedi, 2012; Olivera, 2001; Razi *et al.*, 2010). The temperature index method for snowmelt runoff modeling is a suitable approach in HEC-HMS model (Verdhen *et al.*, 2013) and reliable results are observed by the researchers worldwide (Fazel *et al.*, 2013; Azmat *et al.*, 2017).

The GSMaP_NRT and GSMaP_NOW based simulations show reliable agreement with the observed flow for almost all of the time periods and tested by the researchers worldwide (Okamoto *et al.*, 2005; Kubota *et al.*, 2007). There are some uncertainties in simulations which can be minimized by local calibration of the precipitation estimates (Cheema and Bastiaanssen, 2012; Mashingia *et al.*, 2014; Shiraishi *et al.*, 2009) as self-corrected GSMaP_NRT has been applied over the Indus basin by Sugiura *et al.* (2016). The GSMaP_RNC based simulated flow shows poor results with high over and underestimation as its overestimation in precipitation is proved in tropics by Kotsuki *et al.* (2019). The higher uncertainties are observed for GSMAP_NOW based simulation in this study as higher uncertainties are also observed for GSMaP_NOW precipitation by Kubota *et al.* (2017) which may lead to less accurate results due to decrease in microwave radiometer coverages with 0.5-hour latency. The variations in the peak magnitude and time of observed and simulated flow is also directly linked to the storage and release due to Indian dams on Chenab river. The accuracy of the simulation can be improved by timely adjustment of storage and release of water from the dams into the HEC-HMS model.

***Conclusion*:** The purpose of this study was to develop a flood forecasting system for the transboundary Chenab river by integrating high spatiotemporal GSMaP precipitation estimates with the HEC-HMS model. The results indicated a reliable agreement between the observed and simulated flows for GSMaP_NRT and GSMaP_NOW precipitation estimates for time series simulation, while very poor simulation results are obtained by using GSMaP_RNC precipitation estimates. Due to their high spatiotemporal characteristics and low latency time, the GSMaP_NRT and GSMaP_NOW precipitation estimates can be used in hydrological models for real time flood forecasting. The real time flood forecasting would help to forecast the magnitude and volume of water which would be helpful in flood management in order to minimize the losses.

REFERENCES

Alexakis, D.D., F.-D.K. Mexis, A.-E.K. Vozinaki, I.N. Daliakopoulos and I.K. Tsanis. 2017. Soil moisture content estimation based on Sentinel-1 and auxiliary earth observation products. A hydrological approach. J. Sens. 17:1455.

Anderson, M., Z.-Q. Chen, M. Kavvas and A. Feldman. 2002. Coupling HEC-HMS with atmospheric models for prediction of watershed runoff. J. Hydr. Engg. 7:312-318.

Aonashi, K., J. Awaka, M. Hirose, T. Kozu, T. Kubota, G. Liu, S. Shige, S. Kida, S. Seto and N. Takahashi. 2009. GSMaP passive microwave precipitation retrieval algorithm: Algorithm description and validation. J.Met. Soc. Ser. 87:119-136.

Azmat, M., M.U. Qamar, S. Ahmed, E. Hussain and M. Umair. 2017. Application of HEC-HMS for the event and continuous simulation in high altitude scarcely-gauged catchment under changing climate. Eur. Wat. 57:77-84.

Bhuiyan, H., H. Mcnairn, J. Powers and A. Merzouki. 2017. Application of HEC-HMS in a cold region watershed and use of RADARSAT-2 soil moisture in initializing the model. Hydr. 4:1-9.

Biemans, H., R. Hutjes, P. Kabat, B. Strengers, D. Gerten and S. Rost. 2009. Effects of precipitation uncertainty on discharge calculations for main river basins. J. Hydromet. 10:1011-1025.

Cheema, M.J.M. and W.G. Bastiaanssen. 2012. Local calibration of remotely sensed rainfall from the TRMM satellite for different periods and spatial scales in the Indus Basin. Int. J. Rem. Sen. 33:2603-2627.

Corbari, C. and M. Mancini. 2014. Calibration and validation of a distributed energy–water balance model using satellite data of land surface temperature and ground discharge measurements. J. Hydromet. 15:376-392.

Cydzik, K. and T.S. Hogue. 2009. Modeling postfire response and recovery using the hydrologic engineering center-hydrologic modeling system (HEC-HMS). J. Ame. Wat. Res. Assoc. 45:702-714.

Dariane, A.B., R. Bagheri, F. Karami and M.M. Javadianzadeh. 2020. Developing heuristic multi-criteria auto calibration method for continuous HEC-HMS in snow-affected catchment. Int. J.Riv. Bas. Mang. 18:69-80.

De Silva, M., S. Weerakoon and S. Herath. 2014. Modeling of event and continuous flow hydrographs with HEC–HMS: case study in the Kelani River Basin, Sri Lanka. J. Hydr. Engg. 19:800-806.

Ebert, E.E., J.E. Janowiak and C. Kidd. 2007. Comparison of near-real-time precipitation estimates from satellite observations and numerical models. Bul.Ame. Met. Soc. 88:47-64.

Fazel, K., W.A. Scharffenberg and F.A. Bombardelli. 2013. Assessment of the melt rate function in a temperature index snow model using observed data. J. Hydr. Engg. 19:1275-1282.

Feldman, A.D. 2000. Hydrologic Engineering Centre-Hydrologic Modeling System (HEC-HMS): technical reference manual, US Army Corps of Engineers, Hydrologic Engineering Center.

FFC. 2000. Annual Flood Report, Federal Flood Commission, Ministry of Water and Power of Pakistan. Water and Power Development Authority, Islamabad, Pakistan.

FFC. 2017. Annual Flood Report, Federal Flood Commission, Ministry of Water and Power of Pakistan. Water and Power Development Authority, Islamabad, Pakistan.

García, A., A. Sainz, J.A. Revilla, C. Álvarez, J.A. Juanes and A. Puente. 2008. Surface water resources assessment in scarcely gauged basins in the north of Spain. J. Hydr. 356:312-326.

Ghimire, R., S. Ferreira and J.H. Dorfman. 2015. Flood-induced displacement and civil conflict. Wor. Dev. 66:614-628.

Groisman, P.Y., R.W. Knight, T.R. Karl, D.R. Easterling, B. Sun and J.H. Lawrimore. 2004. Contemporary changes of the hydrological cycle over the contiguous United States: Trends derived from in situ observations. J. Hydromet. 5:64-85.

Gyawali, R. and D.W. Watkins. 2012. Continuous hydrologic modeling of snow-affected watersheds in the Great Lakes basin using HEC-HMS. J. Hydr. Engg. 18:29-39.

Haynes, K., L. Coates, R. Leigh, A. Gissing, J. Mcaneney, A. Handmer, J. Whittaker and S. Opper. 2009. Shelter-in-place versus evacuation in flash flood environments. 49th Annual Floodplain Management Authorities Conference and 6th Biennial Victorian Flood Conference. Albury, Australia. 8:291-303.

HEC. 2015. US Army Corps of Engineers, Hydrologic Modeling System (HEC-HMS). Application Guide: Version 3.1. 0. Institute for Water Resources, Hydrologic Engineering Center, Davis, CA, USA.

Herold, N., L. Alexander, M. Donat, S. Contractor and A. Becker. 2016. How much does it rain over land? Geophy. Res. Let. 43:341-348.

Hersbach, H. and D. Dee. 2016. ERA-5 reanalysis is in production. ECMWF newsletter, number 147, p.7, Spring 2016.7.

Huffman, G.J., D.T. Bolvin, E.J. Nelkin, D.B. Wolff, R.F. Adler, G. Gu, Y. Hong, K.P. Bowman and E.F. Stocker. 2007. The TRMM multisatellite precipitation analysis (TMPA): Quasi-global, multiyear, combined-sensor precipitation estimates at fine scales. J. Hydromet. 8:38-55.

Immerzeel, W.W., F. Pellicciotti and A.B. Shrestha. 2012. Glaciers as a proxy to quantify the spatial distribution of precipitation in the Hunza basin. Moun. Res.Dev. 32:30-38.

Kotsuki, S., K. Kurosawa, S. Otsuka, K. Terasaki and T. Miyoshi. 2019. Global Precipitation Forecasts by Merging Extrapolation-based Nowcast and Numerical Weather Prediction with Locally-optimized Weights. Weat. Fore.

Kubota, T., K. Aonashi, T. Ushio, S. Shige, Y.N. Takayabu, Y. Arai, T. Tashima, M. Kachi and R. Oki. Recent progress in global satellite mapping of precipitation (GSMaP) product. 2017 IEEE International Geoscience and Remote Sensing Symposium (IGARSS), 2017. IEEE: 2712-2715.

Kubota, T., S. Shige, H. Hashizume, K. Aonashi, N. Takahashi, S. Seto, M. Hirose, Y.N. Takayabu, T. Ushio and K. Nakagawa. 2007. Global precipitation map using satellite-borne microwave radiometers by the GSMaP project: Production and validation. IEEE Trans. Geosc-Rem. Sen. 45:2259-2275.

Kwak, Y.-J. and J. Park 2019. Annual Flood Monitoring Using Synchronized Floodwater Index in 2010 Indus River Flood. *Indus River Basin.* Else.

Looney, R. 2012. Economic impacts of the floods in Pakistan. Contemporary south asia. 20:225-241.

Majidi, A. and K. Shahedi. 2012. Simulation of rainfall-runoff process using Green-Ampt method and HEC-HMS model (Case study: Abnama Watershed, Iran). Int. J. Hydra Engg. 1:5-9.

Mallakpour, I. and G. Villarini. 2015. The changing nature of flooding across the central United States. Nat. Clim. Chan. 5:250.

Mashingia, F., F. Mtalo and M. Bruen. 2014. Validation of remotely sensed rainfall over major climatic regions in Northeast Tanzania. Phy. Chem. Ear. Parts A/B/C. 67:55-63.

MMC. 2005. Natural hazard mitigation saves: An independent study to assess the future savings from mitigation activities. Multihazard Mitigation Council. National Institute of Building Sciences, Washington, DC. 68.

Nakayama, T. 2015. Integrated Assessment System Using Process-Based Eco-Hydrology Model for Adaptation Strategy and Effective Water Resources Management. Rem. Sen. Terr. Wat. Cyc.521-535.

OA. 2010. Oxford Analytica. Pakistan: Floods imperil long term prospects, August 24, 2010.

Okamoto, K., T. Iguchi, T. Ushio, N. Takahashi and K. Iwanami. 2005. K, Iwanami, and T. The global satellite mapping of precipitation (GSMaP).Project. Proc. 25th Int. Symp. Geosc. Rem. Sen., Seoul, South Korea, IEEE 3414–3416.

Olivera, F. 2001. Extracting hydrologic information from spatial data for HMS modeling. J. Hydr. Engg. 6:524-530.

Otsuka, S., S. Kotsuki, M. Ohhigashi and T. Miyoshi. 2019. GSMaP RIKEN Nowcast: Global precipitation nowcasting with data assimilation. J. Met. Soc. Japan. Ser. II.

Ouédraogo, W.a.A., J.M. Raude and J.M. Gathenya. 2018. Continuous modeling of the Mkurumudzi River catchment in Kenya using the HEC-HMS conceptual model: Calibration, validation, model performance evaluation and sensitivity analysis. Hydr. 5:44.

Razi, M., J. Ariffin, W. Tahir and N. Arish. 2010. Flood estimation studies using hydrologic modeling system (HEC-HMS) for Johor River, Malaysia. J. App. Sci. 10:930-939.

Schaffenberg, W. 2013. Hydrologic Modeling System HEC-HMS, User Manual: Version 4.0. US Army Corps of Engineers,Hydrologic Engineering Center. 609.

Schaffenberg, W. and M. Fleming. 2006. Hydrologic Modeling System HEC-HMS, User Manual: Version 4.0. US Army Corps of Engineers, Hydrologic Engineering Center.

Shiraishi, Y., K. Fukami and H. Inomata. 2009. The proposal of correction method using the movement of rainfall area on satellite-based rainfall information by analysis in the Yoshino River Basin. Ann. J. Hydra. Engg. 53:385-390.

Simonovic, S. 2009. Managing flood risk, reliability and vulnerability. J. Flo. Ris. Mang. 2:230-231.

Singh, W.R. and M.K. Jain. 2015. Continuous hydrological modeling using soil moisture accounting algorithm in Vamsadhara River basin, India. J. Wat. Res. Hydra. Engg. 4:398-408.

Sintayehu, L. 2015. Application of the HEC-HMS model for runoff simulation of upper blue Nile River Basin. Hydro. Curr. Res. 6:2.

Stefanidis, S. and D. Stathis. 2013. Assessment of flood hazard based on natural and anthropogenic factors using analytic hierarchy process (AHP). Nat. Haz. 68:569-585.

Sturm, M., B. Taras, G.E. Liston, C. Derksen, T. Jonas and J. Lea. 2010. Estimating snow water equivalent using snow depth data and climate classes. J. Hydromet. 11:1380-1394.

Sugiura, A., S. Fujioka, S. Nabesaka, T. Sayama, Y. Iwami, K. Fukami, S. Tanaka and K. Takeuchi. 2014. Challenges on modelling a large river basin with scarce data: A case study of the Indus upper catchment. J. Hydr. Env. Res. 2:59-64.

Sugiura, A., S. Fujioka, S. Nabesaka, M. Tsuda and Y. Iwami. 2016. Development of a flood forecasting system on the upper Indus catchment using IFAS. J. Flo. Ris. Mang. 9:265-277.

Tang, G., Z. Zeng, M. Ma, R. Liu, Y. Wen and Y. Hong. 2017. Can near-real-time satellite precipitation products capture rainstorms and guide flood warning for the 2016 summer in south China? IEEE Geoscience-Rem. Sen. let. 14:1208-1212.

Tapiador, F.J., F.J. Turk, W. Petersen, A.Y. Hou, E. García-Ortega, L.A. Machado, C.F. Angelis, P. Salio, C. Kidd and G.J. Huffman. 2012. Global precipitation measurement: Methods, datasets and applications. Atm. Res. 104:70-97.

Tariq, M.a.U.R. and V.D.N. Giesen. 2012. Floods and flood management in Pakistan. Phy. Chem Ear, Parts A/B/C. 47:11-20.

Tei, S., T. Morozumi, S. Nagai, S. Takano, A. Sugimoto, R. Shingubara, R. Fan, A. Fedorov, T. Gavrilyeva and N. Tananaev. 2019. An extreme flood caused by a heavy snowfall over the Indigirka River basin in Northeastern Siberia. Hydr. Pro.

Teng, F., W. Huang and I. Ginis. 2018. Hydrological modeling of storm runoff and snowmelt in Taunton River Basin by applications of HEC-HMS and PRMS models. Nat. Haz. 91:179-199.

Terzago, S., V. Andreoli, G. Arduini, G. Balsamo, L. Campo, C. Cassardo, E. Cremonese, D. Dolia, S. Gabellani and J. Von Hardenberg. Sensitivity of snow models to the accuracy of the meteorological forcing in a mountain environment. Geophy. Res. Abs, 2019.

Tsujimoto, K., T. Ohta and T. Koike. Validation of satellite precipitation product GSMaP/NRT with ground rain gauges in Cambodia. EGU General Assembly Conference Abstracts, 2014.

UNDP. 2012. Putting Resilience at the Heart of Development: Investing in Prevention and Resilient Recovery. United Nations Development Programme.

Ushio, T., K. Sasashige, T. Kubota, S. Shige, K.I. Okamoto, K. Aonashi, T. Inoue, N. Takahashi, T. Iguchi and M. Kachi. 2009. A Kalman filter approach to the Global Satellite Mapping of Precipitation (GSMaP) from combined passive microwave and infrared radiometric data. J. Met. Soc. Japan. Ser. II. 87:137-151.

Verdhen, A., B.R. Chahar and O.P. Sharma. 2013. Snowmelt runoff simulation using HEC-HMS in a himalayan watershed. World Environmental and Water Resources Congress 2013: Showcasing the Future. 3206-3215.

Verma, A.K., M.K. Jha, R.K.J.P. Mahana and W. Environment. 2010. Evaluation of HEC-HMS and WEPP for simulating watershed runoff using remote sensing and geographical information system. 8:131-144.

Wallner, M., U. Haberlandt and J. Dietrich. 2012. Evaluation of different calibration strategies for large scale continuous hydrological modelling. Advances in Geosciences. 31:67-74.

Xie, P., M. Chen, S. Yang, A. Yatagai, T. Hayasaka, Y. Fukushima and C. Liu. 2007. A gauge-based analysis of daily precipitation over East Asia. J. Hydromet. 8:607-626.

Xu, L., R. Myneni, F. Chapin Iii, T.V. Callaghan, J. Pinzon, C.J. Tucker, Z. Zhu, J. Bi, P. Ciais and H. Tømmervik. 2013. Temperature and vegetation seasonality diminishment over northern lands. Nat. Clim. Chan.. 3:581.

Yang, T., S. Yang, J. Ho, G. Lin, G. Hwang and C. Lee. 2015. Flash flood warnings using the ensemble precipitation forecasting technique: A case study on forecasting floods in Taiwan caused by typhoons. J. Hydr. 520:367-378.

[Received 10 Feb 2020; Accepted 06 Jul 2020; Published (online) 1 Sept 2020]